



# CHARACTERIZATION OF GRAPHENE OXIDE SYNTHESIZED THROUGH A MODIFIED HUMMERS METHOD

## CARACTERIZACIÓN DE ÓXIDO DE GRAFENO SINTETIZADO MEDIANTE UN MÉTODO DE HUMMERS MODIFICADO

Wilson Navas-Pinto<sup>1,\*</sup>, Duncan E. Cree<sup>3</sup>, Lee D. Wilson<sup>4</sup>,  
Germán Omar Barrionuevo<sup>1,5</sup>, Xavier Sánchez-Sánchez<sup>1</sup>, Héctor Calvopiña<sup>1</sup>

Received: 08-10-2024, Received after review: 25-03-2025, Accepted: 27-03-2025, Published: 01-07-2025

### Abstract

Graphene oxide (GO) has garnered significant interest due to its exceptional and tunable properties, which make it a promising candidate for a wide range of engineering applications, including composite material fabrication and water treatment. In this study, GO was synthesized from graphite flakes using a modified Hummers method involving a reduced amount of sulfuric acid. The resulting material was characterized using scanning electron microscopy (SEM), Fourier transform infrared spectroscopy (FTIR), and X-ray photoelectron spectroscopy (XPS). These techniques enabled a clear differentiation between the morphology of the synthesized GO and that of the original graphite. The GO exhibited a substantially altered structure, with increased thickness likely due to the incorporation of oxygen-containing functional groups on its basal plane.

### Resumen

El óxido de grafeno ha despertado un creciente interés debido a sus propiedades únicas y potencialmente ajustables, las cuales abarcan aplicaciones que van desde la fabricación de materiales compuestos hasta el tratamiento de aguas. Por esta razón, se desarrolló un proceso de síntesis de óxido de grafeno basado en el método de Hummers con una reducción en la cantidad de ácido sulfúrico empleada. El material obtenido fue caracterizado mediante diferentes técnicas, incluyendo microscopía electrónica de barrido (MEB), espectroscopía infrarroja transformada de Fourier (IR-TF) y espectrometría fotoelectrónica por rayos X (XPS). Estas técnicas experimentales permitieron distinguir las diferencias morfológicas entre el óxido de grafeno sintetizado y el grafito utilizado como precursor. Adicionalmente, se determinó la composición química del polvo obtenido, así como la relación entre carbono y oxígeno, con el fin de evaluar su viabilidad para aplicaciones específicas. Se observó que la morfología del óxido de grafeno difiere significativamente de la del grafito de partida. En particular, el espesor de las láminas de óxido de grafeno se incrementó debido a la incorporación de grupos funcionales oxigenados en el plano basal.

<sup>1,\*</sup>Department of Energy and Mechanical Sciences, Universidad de las Fuerzas Armadas ESPE, Quito, Ecuador   
Corresponding Author ✉: [wnavas1@espe.edu.ec](mailto:wnavas1@espe.edu.ec)

<sup>2</sup>Department of Mechanical Engineering University of Saskatchewan, Saskatoon, Canadá

<sup>3</sup>Department of Mechanical Engineering, McMaster University, Hamilton, Canadá

<sup>4</sup>Department of Chemistry, University of Saskatchewan, Saskatoon, Canadá

<sup>5</sup>Engineering Department, Universidad Católica de Uruguay, Montevideo, Uruguay

Suggested citation: Navas-Pinto, W.; Cree, D.; Wilson, L.; Barrionuevo, G.; Sánchez-Sánchez, X. and Calvopiña, H. "Characterization of graphene oxide synthesized through a modified Hummers method," *Ingenius, Revista de Ciencia y Tecnología*, N.º 34, pp. 31-42, 2025, DOI: <https://doi.org/10.17163/ings.n34.2025.03>.

FTIR analysis confirmed the presence of characteristic functional groups such as hydroxyl, carbonyl, and carboxyl. XPS analysis revealed that the elemental composition of the synthesized GO consisted of approximately 69.7% carbon and 29.9% oxygen, with a trace amount of sulfur attributed to the reagents used in the synthesis. The observed changes in morphology and composition suggest the successful synthesis of GO with potential for functionalization and application in diverse engineering contexts.

**Keywords:** Graphene oxide, synthesis, functional groups, FTIR, SEM, XPS

El espectro FTIR del óxido de grafeno confirmó la presencia de diversos grupos funcionales, como el hidroxilo (-OH), carbonilo (C=O) y carboxilo (-COOH). Por su parte, la espectroscopía XPS reveló que la composición química del óxido de grafeno obtenido fue de 69,7 % de carbono y 29,9 % de oxígeno, con una traza mínima de azufre atribuida a los reactivos empleados durante el proceso de síntesis.

**Palabras clave:** óxido de grafeno, síntesis, grupos funcionales, IR-TF, MEB, XPS

## 1. Introduction

Graphene oxide (GO) consists of a single-atom-thick hexagonal carbon basal plane decorated with randomly distributed oxygen-containing functional groups [1, 2], as illustrated in Figure 1. Previous studies have reported that the thickness of GO typically ranges between 0.7 and 1.6 nm [3, 4] while its lateral dimensions can vary significantly from a few nanometers to several micrometers [1], [5].

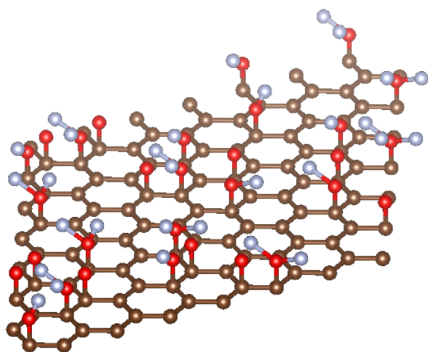


**Figure 1.** Schematic representation of the graphene oxide (GO) structure

Numerous studies have been conducted to assess the feasibility of graphene oxide (GO) in a broad range of applications, owing to its high surface area [6], favorable mechanical properties [7, 8], the presence of diverse oxygen-containing functional groups [9–11], and even its potential antibacterial activity [12–14]. As a result, GO has been explored for use inflexible electronic sensors [15, 16], supercapacitors [17–19], energy storage and conversion systems [20, 21], biomedical devices [22, 23], composite materials [24, 25], water treatment technologies [26], and microbial activity control [27].

For instance, Liang et al. [16] developed reduced graphene oxide (rGO) humidity sensors and reported rapid response and recovery times, attributed to the inhibition of water molecule aggregation due to the structural characteristics of rGO. Similarly, Kerli et al. [17] synthesized silver-doped rGO polyaniline (PANI) composites and evaluated their specific capacitance, observing a maximum improvement of 17% compared to conventional materials. Eftekhari et al. [21] investigated the fabrication of GO-based membranes for electrochemical energy storage, highlighting the superior diffusion of water molecules through GO, which enhanced membrane performance in acidic electrolyte environments. GO has also been incorporated into polymer matrices at low concentrations, resulting in improved mechanical properties compared to neat polymer samples [24]. In biomedical applications, GO has demonstrated potential for promoting periodontal tissue regeneration and reducing inflammation when

integrated into collagen scaffolds [23]. Additionally, GO-based membranes have been tested for water filtration, where the incorporation of GO into chitosan enhanced both water permeability and dye rejection properties [26]. Regarding antimicrobial activity, Yu et al. [27] evaluated the effectiveness of different GO solutions in controlling the proliferation of *Streptococcus mutans* and found that GO particle size had a direct influence on antimicrobial efficacy.

The synthesis of graphene oxide (GO) involves a strong oxidation process in which graphite flakes are treated with various oxidizing agents as raw materials [11], [28]. This procedure results in the formation of graphite oxide, from which GO is subsequently obtained through an exfoliation or sonication step that separates individual layers to yield a single-layered material [21], [29]. The mechanical properties of GO are highly dependent on its synthesis conditions, which influence its structure, degree of oxidation, chemical composition, and carbon-to-oxygen (C/O) ratio. Several studies have reported the mechanical performance of monolayer GO; for instance, its tensile strength has been measured at approximately  $77 \pm 20$  MPa, and its elastic modulus falls within the range of 150 to 250 GPa [2], [30]. In comparison, pristine graphene exhibits significantly higher mechanical properties, with a tensile strength ranging from 50 to 60 GPa and an elastic modulus close to 1 TPa [31]. Despite its relatively lower mechanical strength, GO exhibits superior chemical reactivity due to the presence of functional groups on its basal plane, which makes it highly amenable to bonding with other materials. This reactivity facilitates the development of advanced composite and hybrid materials [32, 33].

Graphene oxide (GO) has been synthesized using various methods, each differing primarily in the type and concentration of oxidizing agents employed [34–38], as illustrated in Figure 2.

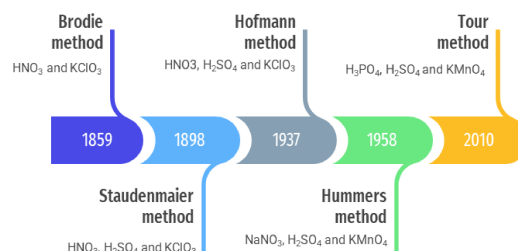


**Figure 2.** Timeline of GO synthesis methods and their corresponding oxidizing agents

In 1859, Brodie [34] conducted the first documented attempt to oxidize graphite. For this purpose, a solution was prepared using a 3:1 ratio of potassium chlorate ( $KClO_3$ ) and nitric acid ( $HNO_3$ ), which was then mechanically stirred with a measured quantity of graphite. Once a homogeneous mixture was achieved,

the solution was heated to 60 °C and continuously stirred for 72 hours or until the evolution of yellow fumes had ceased. Following the reaction, multiple washing steps were carried out by adding deionized water and decanting the mixture to eliminate any residual unreacted reagents. The resulting substance, initially referred to as graphitic acid, was found to be partially soluble in deionized water, but insoluble in both pure water and acidic solutions.

Staundemaier [35] reported an alternative method for synthesizing graphene oxide (GO) by incorporating sulfuric acid ( $H_2SO_4$ ) into the original solution developed by Brodie. In this procedure, a mixture of  $H_2SO_4$  and nitric acid ( $HNO_3$ ) in a 1:3 volume ratio was stirred until the emission of fumes was observed. The fuming mixture was then added to graphite flakes, which were maintained in an ice bath and stirred for 30 minutes. Subsequently, potassium chlorate ( $KClO_3$ ) was slowly added to prevent a rapid increase in temperature. The solution was then transferred to ambient conditions and stirred continuously for an additional 96 hours. Finally, several decantation and washing steps were carried out using hydrochloric acid (HCl) and demineralized water to remove any supernatant.

Similarly, Hofmann and König [36] carried out an oxidation process on graphite flakes, introducing temperature variation as a key parameter during the synthesis. Initially, a solution consisting of sulfuric acid ( $H_2SO_4$ ) and nitric acid ( $HNO_3$ ) in a 1:3 volume ratio was prepared and placed in an ice bath to suppress gas evolution. Graphite flakes were then added gradually, with continuous stirring maintained throughout the cooling stage. Subsequently, potassium chlorate ( $KClO_3$ ) was slowly introduced over a period of approximately 30 minutes. The resulting mixture was then subjected to magnetic stirring for 96 hours at room temperature. Finally, a hydrochloric acid (HCl) solution at 5% by volume was added to eliminate residual sulfate ions, followed by multiple washing steps with deionized water.

In 1958, Hummers and Offeman [37] introduced a direct method for synthesizing graphene oxide (GO) using sulfuric acid ( $H_2SO_4$ ), sodium nitrate ( $NaNO_3$ ), and potassium permanganate ( $KMnO_4$ ) as oxidizing agents. In this procedure, a beaker was placed in an ice bath prior to the addition of 100 g of graphite flakes, 50 g of  $NaNO_3$ , and 2.3 liters of concentrated  $H_2SO_4$ . The mixture was vigorously stirred until a homogeneous dispersion was achieved. Subsequently, 300 g of  $KMnO_4$  was gradually added while maintaining the temperature below 20 °C. The reaction mixture was then transferred to an oil bath at 35 °C and stirred for 30 minutes. This step was followed by the addition of 4.6 liters of demineralized water, which induced vigorous effervescence and elevated the temperature to approximately 98 °C. Next, 14 liters of a solution composed of warm water and 3% hydrogen peroxide

( $H_2O_2$ ) were added to neutralize any remaining oxidizing agents. The final steps involved repeated washing with deionized water, followed by centrifugation and vacuum drying of the resulting slurry at 40 °C.

In 2010, Marcano et al. [38] developed a modified synthesis route for graphene oxide (GO) based on the Hummers method. In this approach, the amount of potassium permanganate ( $KMnO_4$ ) was increased, and the reaction was carried out using a 9:1 volumetric mixture of sulfuric acid ( $H_2SO_4$ ) and phosphoric acid ( $H_3PO_4$ ). This modification effectively suppressed the generation of hazardous fumes and yielded GO with an increased oxygen content.

In addition to conventional methods, several novel approaches have been explored to synthesize graphene oxide (GO) powder. For instance, Chen et al. [39] proposed a modified version of the Hummers method in which sodium nitrate ( $NaNO_3$ ) was excluded from the reaction mixture to prevent the formation of potentially toxic nitrogen-based gases. This alternative protocol effectively oxidized graphite, yielding results comparable to those obtained with the original Hummers method.

Given the extensive research dedicated to synthesizing graphene oxide (GO) from graphite and its potential applications in future engineering technologies, this study focuses on the characterization and morphological analysis of GO powder synthesized via a modified Hummers method. Comprehensive characterization of the resulting material was carried out using scanning electron microscopy (SEM), Fourier-transform infrared spectroscopy (FTIR), and X-ray photoelectron spectroscopy (XPS).

## 2. Materials and Methods

### 2.1. Materials

Graphite powder (325 mesh, 99.9995% metals basis) was obtained from Thermo Scientific Chemicals. Potassium permanganate ( $KMnO_4$ ), sodium nitrate ( $NaNO_3$ ), and concentrated sulfuric acid ( $H_2SO_4$ ) were supplied by Fisher Chemical<sup>TM</sup>. All reagents were used as received without further purification.

### 2.2. GO Synthesis

Graphene oxide (GO) was synthesized using a modified Hummers method, in which the amount of sulfuric acid ( $H_2SO_4$ ) was reduced to minimize the residual sulfur content in the final product. The procedure began by adding 5 g of graphite powder, 2.5 g of sodium nitrate ( $NaNO_3$ ), and 105 mL of concentrated  $H_2SO_4$  to a beaker. The quantity of sulfuric acid was decreased by approximately 10% compared to the original Hummers method [37] to assess the extent to which this modification reduces the presence of residual sulfur in the

synthesized GO [40]. The resulting mixture was magnetically stirred for 45 minutes until a homogeneous solution was obtained. It was then placed in an ice bath and stirred for an additional hour. Subsequently, 15 g of potassium permanganate ( $KMnO_4$ ), was gradually added with continuous stirring, carefully maintaining the temperature to prevent a rapid rise. The solution was then transferred to a cold-water bath at approximately 15 °C and stirred for another 30 minutes, with ice added as necessary to keep the temperature below 20 °C. The reaction mixture was next placed in a warm water bath (approximately 35 °C), and 230

mL of deionized water was added slowly in small increments. After the complete addition, the solution was transferred to an oil bath at 98 °C and stirred for 20 minutes. This was followed by the addition of 400 mL of distilled water, which caused a visible color change from dark brown to light brown, with stirring continued for an additional 20 minutes. Subsequently, 50 mL of hydrogen peroxide ( $H_2O_2$ ) was introduced to terminate the reaction. Finally, the suspension was stirred at room temperature for 12 hours to complete the oxidation process, see figure 3.

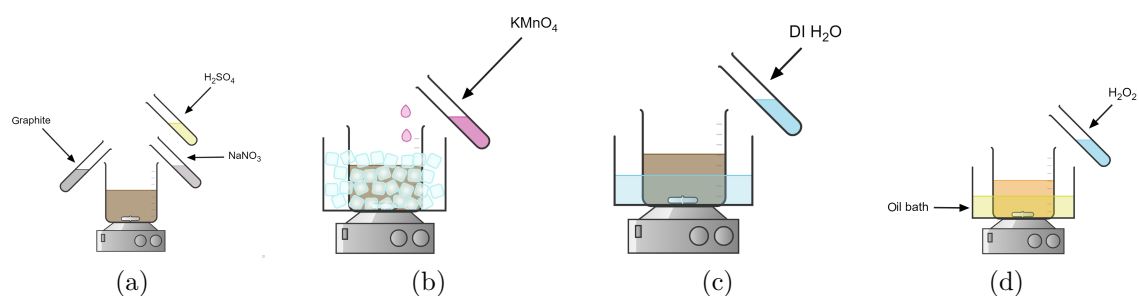


**Figure 3.** Schematic representation of the GO synthesis process. a) Initial stage involving the addition of the primary reagents. b) Ice bath stage, during which potassium permanganate is gradually introduced. c) Addition of deionized water to the reaction mixture. d) Final stage involving the addition of hydrogen peroxide to complete the oxidation process

Once the synthesis was complete, a multi-step purification process was carried out to remove unreacted chemicals and ensure the appropriate purity of the synthesized graphene oxide (GO). Each initial purification stage involved the addition of 500 mL of deionized water, followed by stirring for 60 minutes. The suspension was then allowed to precipitate, and the supernatant was carefully decanted. This stage was repeated four times, during which a progressive darkening of the solution was observed. Subsequently, 200 mL of a 30% (v/v) hydrochloric acid (HCl) solution was added and stirred for 60 minutes. After precipitation, the supernatant was again removed. This was followed by the addition of 200 mL of ethanol ( $C_2H_5OH$ ), which was stirred for an additional hour before decanting. Two final washing steps were conducted using 400 mL of deionized water in each cycle to complete the purification. The resulting solution was then poured into Petri dishes to form thin films approximately 1–2 mm thick and dried in a vacuum oven at 30 °C until dry membranes were obtained. These membranes were manually ground and sieved using a 100-mesh screen to ensure a uniform particle size distribution. The yield of each synthesis batch ranged from 6.8 to 7.2 g of GO powder, with minor variations attributed to unintentional losses during supernatant removal.

### 2.3. GO characterization

To confirm the successful synthesis of graphene oxide (GO) powder, a series of characterization techniques were employed. Fourier-transform infrared (FT-IR) spectroscopy was used to assess the presence of characteristic functional groups [41, 42]. For this purpose, both the starting graphite powder and the synthesized GO powder were analyzed using a Bio-RAD FTS-40 infrared spectrometer [43]. Each sample was mixed with potassium bromide (KBr) in a 1:10 weight ratio. In addition, scanning electron microscopy (SEM) was used to compare the morphology of the two materials. SEM images were acquired using a JEOL JSM-6010 LV microscope operating at an acceleration voltage of 10 kV. Image processing software was utilized to measure particle dimensions, and the average particle size was determined using statistical analysis tools. X-ray photoelectron spectroscopy (XPS) was conducted to evaluate the degree of oxidation in the GO samples via the carbon-to-oxygen (C/O) ratio. Measurements were performed using a Kratos AXIS Supra system equipped with an Al K- $\alpha$  monochromator (1486,66 eV), operating at an acceleration voltage of 15 kV and an emission current of 15 mA. Survey scans were recorded in the range of 0–1200 eV with a step size of 1eV and a pass energy of 160 eV. The acquired spectra were analyzed using CASA XPS software. The density

of the GO powder was measured using a Micromeritics AccuPyc 1340 helium gas pycnometer. Prior to analysis, the instrument was calibrated by placing a stainless-steel sphere of known volume ( $V_C$ ) in the sample chamber. The GO powder was then weighed ( $m_S$ ) and placed in the chamber, which was subsequently filled with helium until reaching a pressure of 110 MPa ( $P_2$ ). Simultaneously, a second steel sphere with known volume ( $V_R$ ) was placed in the reference chamber, and its pressure ( $P_1$ ) was recorded. The sample volume was calculated using Equation (1), and the process was repeated five times to ensure accuracy. Reported values represent the average of these measurements.

$$V_S = V_C - V_R \left( \frac{P_1}{P_2} - 1 \right) \quad (1)$$

Finally, the density of the GO powder was calculated using Equation (2).

$$\rho_{GO} = \frac{m_S}{V_S} \quad (2)$$

### 3. Results and Discussion

#### 3.1. FT-IR Spectral Analysis

The FT-IR spectra of both the raw graphite powder and the synthesized graphene oxide (GO) are presented in Figure 4. The spectrum of graphite (light gray) exhibits an almost constant absorbance between 0.71 and 1, with no prominent peaks, indicating the chemically inert nature of graphite [44,45]. In contrast, the FT-IR spectrum of GO displays several characteristic absorption bands, confirming the presence of various oxygen-containing functional groups on the basal plane of the material [9], [46]. A broad absorption band centered around  $3300 \text{ cm}^{-1}$  corresponds to the  $C-OH$  stretching vibration, indicating the presence of hydroxyl groups [46,47]. The band near  $2300 \text{ cm}^{-1}$  corresponds to  $CH_2$  stretching vibrations [48]. A well-defined peak observed at approximately  $1700 \text{ cm}^{-1}$  is attributed to  $C=O$  stretching, indicative of carbonyl groups [44,47]. Similarly, the peak around  $1600 \text{ cm}^{-1}$  is associated with  $C=C$  stretching vibrations [47], [49]. The absorption band at  $1050 \text{ cm}^{-1}$  is related to  $C-O$  and  $C-C$  stretching modes [45], while the band near  $700 \text{ cm}^{-1}$  corresponds to  $O-H$  out-of-plane bending [48,49].

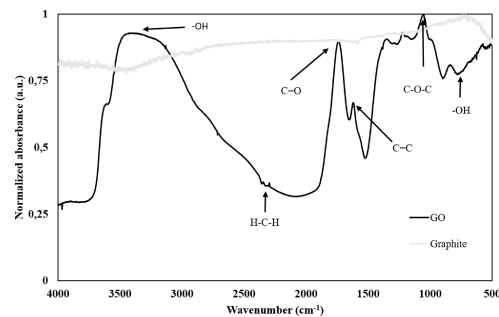


Figure 4. FTIR spectra of graphite and GO powder

#### 3.2. SEM Analysis

Figure 5a displays the SEM micrograph of the as-received graphite powder at  $500\times$  magnification, while Figure 5b presents the micrograph of the ground graphene oxide (GO) obtained under the same conditions. The graphite particles exhibit uniformly sized structures with smooth surfaces. In contrast, the GO sample shows a broader distribution of particle sizes, ranging approximately from  $60$  to  $200 \mu\text{m}$ . Furthermore, GO particles exhibit more irregular and rougher surface morphologies compared to the pristine graphite. The increased thickness observed in the GO particles is likely attributed to the incorporation of oxygen-containing functional groups on the basal plane [5], [50,51].

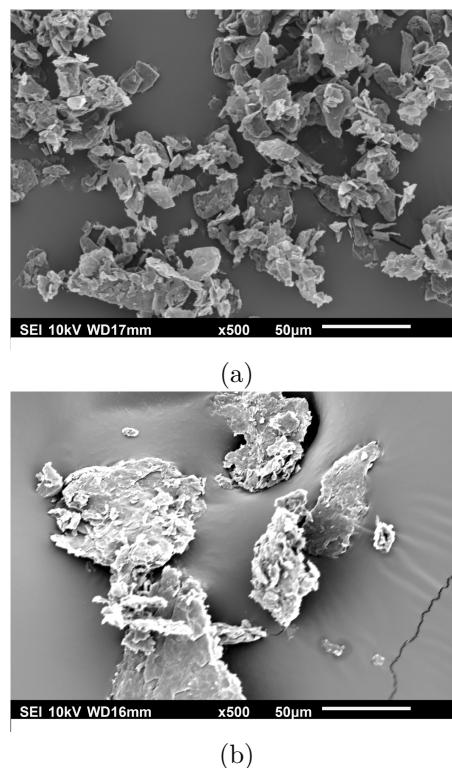
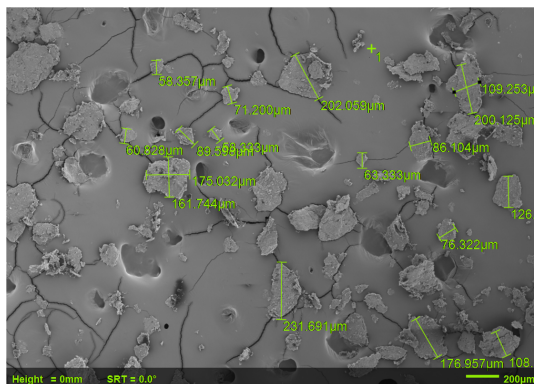
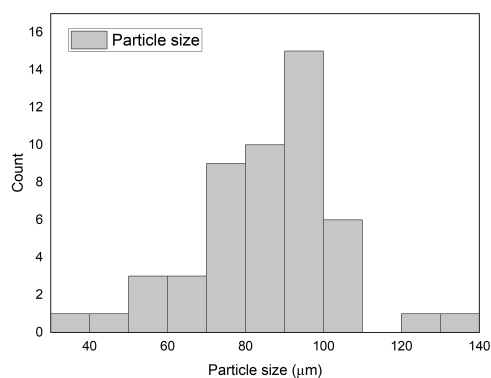


Figure 5. SEM micrographs a) graphite powder 500x, b) synthesized GO 500x

Numerous studies have evaluated the influence of reinforcement particle size on the mechanical properties of composite materials [52, 53]. To determine the average particle size of the synthesized graphene oxide (GO), a scanning electron microscopy (SEM) image captured at  $60\times$  magnification was analyzed, as shown in Figure 6. The dimensions of all visible particles were measured, and a histogram illustrating the particle size distribution is presented in Figure 7. Based on the measurements, the average particle size was calculated to be  $86.144 \pm 11.47 \mu\text{m}$ .



**Figure 6.** SEM micrograph of GO at  $60\times$  magnification, used for particle size analysis

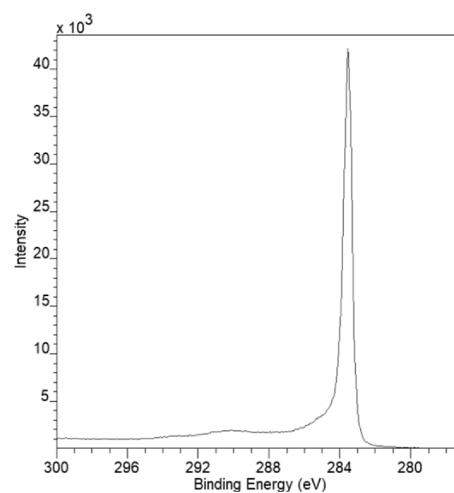


**Figure 7.** Histogram showing the particle size distribution of GO

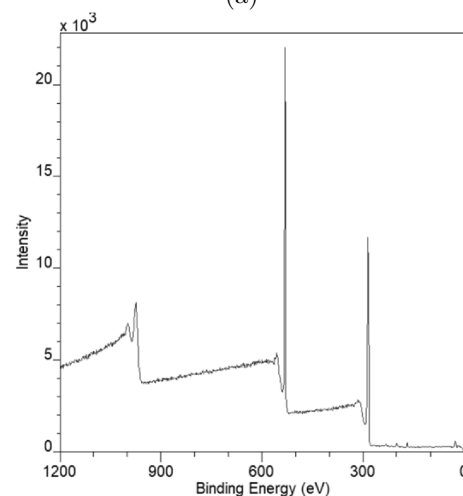
### 3.3. XPS Analysis

Figures 8a and 8b present the X-ray photoelectron spectroscopy (XPS) spectra of pristine graphite and the synthesized graphene oxide (GO), respectively. In the case of graphite, a prominent peak appears at approximately 283 eV, corresponding to the C1s peak. The elemental composition of the graphite sample was determined to be approximately 99% carbon and 1% oxygen. The elevated oxygen content, compared to the

material datasheet, is likely attributed to exposure to atmospheric conditions prior to analysis [54]. In contrast, the GO spectrum exhibits several distinct peaks. Alongside the C1s peak, characteristic oxygen-related signals are observed at around 520 eV and 980 eV, corresponding to the O1s and O KLL transitions, respectively. The elemental composition of the synthesized GO was found to be approximately 69.7% carbon, 29.9% oxygen, and a trace amount of sulfur (0.4%), resulting in a carbon-to-oxygen (C/O) ratio of 2.3. This value falls within the range reported in the literature, typically between 1.8 [10] and 2.77 [55], for GO synthesized via Hummers-based methods.



(a)



(b)

**Figure 8.** XPS spectra of a) graphite and b) synthesized GO

High-resolution scans were acquired with a step size of 50 meV to further characterize the synthesized graphene oxide (GO), as illustrated in Figure 9. The spectra were deconvoluted using CASA XPS software, revealing four prominent peaks located at approximately 284, 286, 288, and 289 eV. These peaks cor-

respond to  $sp^2$  hybridized carbon  $C = C$ , epoxy/hydroxyl groups, carbonyl functionalities, and carboxylates, respectively. Notably, the latter three peaks represent carbon atoms bonded to oxygen-containing functional groups, which collectively account for approximately 47% of the total carbon content in the GO sample. In contrast, the first peak corresponds to carbon atoms bonded exclusively to other carbon atoms.

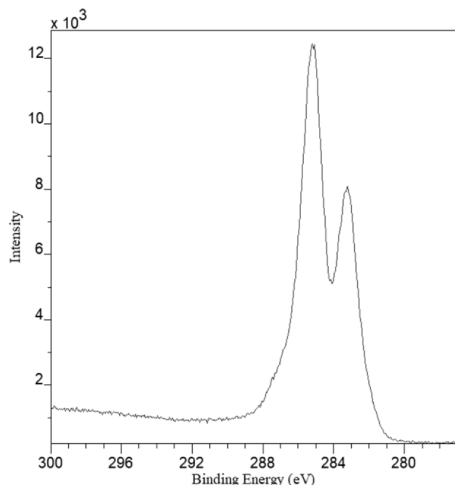


**Figure 9.** High-resolution XPS spectrum of the synthesized GO

### 3.4. Density Measurement

The graphene oxide (GO) sample was first weighed, yielding a consistent mass of 4.775 g across five repeated measurements. Following volume determination, the density of the synthesized GO powder was calculated to be  $2,084 \pm 0,03 \text{ g/cm}^3$ .

## 4. Conclusions

In this study, graphene oxide (GO) was successfully synthesized using a modified Hummers method, and the resulting material was thoroughly characterized to evaluate its potential for engineering applications. The main conclusions are as follows:

Graphene oxide (GO) can be synthesized using various methods employing different ratios of oxidizing agents. The Hummers method is one of the most widely used; however, its reliance on concentrated sulfuric acid often results in trace sulfur contamination in the final product. To mitigate this issue, the present study adopted a modified synthesis protocol in which the amount of sulfuric acid was reduced by approximately 10%.

The FT-IR spectrum of the synthesized GO exhibited characteristic absorption bands at 3300, 2300, 1700, 1600, 1050 and  $700 \text{ cm}^{-1}$ , confirming the success

of the synthesis process. These peaks correspond to hydroxyl ( $-OH$ ) groups,  $CH_2$  stretching vibrations, carbonyl ( $C=O$ ) groups,  $C=C$  stretching, carboxylate ( $O-O-C$ ) groups, and out-of-plane  $O-H$  bending, respectively.

SEM analysis revealed pronounced morphological differences between pristine graphite and the synthesized GO. The GO displayed a more irregular and rougher surface, along with increased thickness, attributed to the presence of oxygen-containing functional groups.

XPS analysis revealed that the elemental composition of the synthesized GO was approximately 69.7% carbon, 29.9% oxygen, and 0.4% sulfur, resulting in a carbon-to-oxygen (C/O) ratio of 2.3.

High-resolution XPS spectra revealed that approximately 47% of the carbon atoms in the synthesized GO were bonded to oxygen-containing functional groups, while the remaining carbon atoms were bonded exclusively to other carbon atoms within the graphene lattice.

The presence of oxygen-containing functional groups enhances the potential of GO for chemical bonding with polymer matrices, particularly those containing epoxide groups, thereby improving the mechanical performance of the resulting composites. Furthermore, the particle size of the synthesized GO suggests its suitability as an effective reinforcing agent in polymer matrix composites.

The density of the synthesized graphene oxide (GO) powder was determined to be  $2.084 \pm 0,03 \text{ g/cm}^3$  using helium gas pycnometry.

## Contributor Roles

- **Wilson Navas-Pinto:** Data curation, formal analysis, investigation, methodology, writing – original draft.
- **Duncan E. Cree:** Conceptualization, formal analysis, funding acquisition, project administration, resources, supervision, validation, writing – review and editing.
- **Lee D. Wilson:** Conceptualization, formal analysis, funding acquisition, project administration, resources, supervision, validation, writing – review and editing.
- **Germán Omar Barrionuevo:** Data curation, methodology, investigation, software, visualization, writing – original draft.
- **Xavier Sánchez-Sánchez:** Formal analysis, resources, software, methodology, validation, visualization, writing – original draft.

- **Héctor Calvopiña:** Methodology, project administration, software, visualization, writing – original draft, writing – review and editing.

## References

- [1] K. Gao, *Graphene Oxide: Reduction Recipes, Spectroscopy, and Applications*. Springer International Publishing, 2015. [Online]. Available: <https://doi.org/10.1007/978-3-319-15500-5>
- [2] J. W. Suk, R. D. Piner, J. An, and R. S. Ruoff, “Mechanical properties of monolayer graphene oxide,” *ACS Nano*, vol. 4, no. 11, pp. 6557–6564, Oct. 2010. [Online]. Available: <https://doi.org/10.1021/nn101781v>
- [3] S. Stankovich, D. A. Dikin, R. D. Piner, K. A. Kohlhaas, A. Kleinhammes, Y. Jia, Y. Wu, S. T. Nguyen, and R. S. Ruoff, “Synthesis of graphene-based nanosheets via chemical reduction of exfoliated graphite oxide,” *Carbon*, vol. 45, no. 7, pp. 1558–1565, Jun. 2007. [Online]. Available: <https://doi.org/10.1016/j.carbon.2007.02.034>
- [4] M. Moazzami Gudarzi and F. Sharif, “Enhancement of dispersion and bonding of graphene-polymer through wet transfer of functionalized graphene oxide,” *Express Polymer Letters*, vol. 6, no. 12, pp. 1017–1031, 2012. [Online]. Available: <http://dx.doi.org/10.3144/expresspolymlett.2012.107>
- [5] K. A. Mkhoyan, A. W. Contryman, J. Silcox, D. A. Stewart, G. Eda, C. Mattevi, S. Miller, and M. Chhowalla, “Atomic and electronic structure of graphene-oxide,” *Nano Letters*, vol. 9, no. 3, pp. 1058–1063, Feb. 2009. [Online]. Available: <https://doi.org/10.1021/nl8034256>
- [6] W. Zięba, K. Jurkiewicz, A. Burian, M. Pawlyta, S. Boncel, G. S. Szymański, J. Kubacki, P. Kowalczyk, K. Krukiewicz, A. Furuse, K. Kaneko, and A. P. Terzyk, “High-surface-area graphene oxide for next-generation energy storage applications,” *ACS Applied Nano Materials*, vol. 5, no. 12, pp. 18 448–18 461, Dec. 2022. [Online]. Available: <http://dx.doi.org/10.1021/acsnm.2c04281>
- [7] X. Mu, X. Wu, T. Zhang, D. B. Go, and T. Luo, “Thermal transport in graphene oxide – from ballistic extreme to amorphous limit,” *Scientific Reports*, vol. 4, no. 1, Jan. 2014. [Online]. Available: <https://doi.org/10.1038/srep03909>
- [8] X. Shen, X. Lin, J. Jia, Z. Wang, Z. Li, and J.-K. Kim, “Tunable thermal conductivities of graphene oxide by functionalization and tensile loading,” *Carbon*, vol. 80, pp. 235–245, Dec. 2014. [Online]. Available: <https://doi.org/10.1016/j.carbon.2014.08.062>
- [9] Z. Li, R. J. Young, R. Wang, F. Yang, L. Hao, W. Jiao, and W. Liu, “The role of functional groups on graphene oxide in epoxy nanocomposites,” *Polymer*, vol. 54, no. 21, pp. 5821–5829, Oct. 2013. [Online]. Available: <https://doi.org/10.1016/j.polymer.2013.08.026>
- [10] C. Botas, P. Álvarez, P. Blanco, M. Granda, C. Blanco, R. Santamaría, L. J. Romasanta, R. Verdejo, M. A. López-Manchado, and R. Menéndez, “Graphene materials with different structures prepared from the same graphite by the hummers and brodie methods,” *Carbon*, vol. 65, pp. 156–164, Dec. 2013. [Online]. Available: <https://doi.org/10.1016/j.carbon.2013.08.009>
- [11] R. K. Singh, R. Kumar, and D. P. Singh, “Graphene oxide: strategies for synthesis, reduction and frontier applications,” *RSC Advances*, vol. 6, no. 69, pp. 64 993–65 011, 2016. [Online]. Available: <https://doi.org/10.1039/C6RA07626B>
- [12] S. Jaworski, B. Strojny-Cieślak, M. Wierzbicki, M. Kutwin, E. Sawosz, M. Kamaszewski, A. Matuszewski, M. Sosnowska, J. Szczepaniak, K. Daniluk, A. Lange, M. Pruchniewski, K. Zawadzka, M. Łojkowski, and A. Chwalibog, “Comparison of the toxicity of pristine graphene and graphene oxide, using four biological models,” *Materials*, vol. 14, no. 15, p. 4250, Jul. 2021. [Online]. Available: <https://doi.org/10.3390/ma14154250>
- [13] P. Kumar, P. Huo, R. Zhang, and B. Liu, “Antibacterial properties of graphene-based nanomaterials,” *Nanomaterials*, vol. 9, no. 5, p. 737, May 2019. [Online]. Available: <https://doi.org/10.3390/nano9050737>
- [14] N. Mushahary, A. Sarkar, F. Basumatary, S. Brahma, B. Das, and S. Basumatary, “Recent developments on graphene oxide and its composite materials: From fundamentals to applications in biodiesel synthesis, adsorption, photocatalysis, supercapacitors, sensors and antimicrobial activity,” *Results in Surfaces and Interfaces*, vol. 15, p. 100225, May 2024. [Online]. Available: <https://doi.org/10.1016/j.rsurfi.2024.100225>
- [15] S. Wang, H. Yan, H. Zheng, Y. He, X. Guo, S. Li, and C. Yang, “Fast response humidity sensor based on chitosan/graphene oxide/tin dioxide composite,” *Sensors and Actuators B: Chemical*, vol. 392, p. 134070, Oct. 2023. [Online]. Available: <https://doi.org/10.1016/j.snb.2023.134070>
- [16] T. Liang, W. Hou, J. Ji, and Y. Huang, “Wrinkled reduced graphene oxide humidity sensor with fast

- response/recovery and flexibility for respiratory monitoring,” *Sensors and Actuators A: Physical*, vol. 350, p. 114104, Feb. 2023. [Online]. Available: <https://doi.org/10.1016/j.sna.2022.114104>
- [17] S. Kerli, S. Bhardwaj, W. Lin, and R. K. Gupta, “Silver-doped reduced graphene oxide/Pani composite synthesis and their supercapacitor applications,” *Journal of Organometallic Chemistry*, vol. 995, p. 122725, Aug. 2023. [Online]. Available: <https://doi.org/10.1016/j.jorganchem.2023.122725>
- [18] S. Nagarani, G. Sasikala, M. Yuvaraj, S. Balachandran, R. Dhilip Kumar, and M. Kumar, “Cost effective, metal free reduced graphene oxide sheet for high performance electrochemical capacitor application,” *Materials Science and Engineering: B*, vol. 284, p. 115852, Oct. 2022. [Online]. Available: <https://doi.org/10.1016/j.mseb.2022.115852>
- [19] S. Nagarani, J.-H. Chang, M. Yuvaraj, S. Balachandran, M. Kumar, and S. Kanimozhi, “Well-organized metal-free chemically reduced graphene oxide sheets as electrocatalysts for enhanced oxygen reduction reactions in alkaline media,” *Materials Letters*, vol. 357, p. 135705, Feb. 2024. [Online]. Available: <https://doi.org/10.1016/j.matlet.2023.135705>
- [20] J. A. Arévalo, J. E. Alfonso, O. J. Suárez, J. J. Olaya, and L. C. Moreno-Aldana, “Growth and physical-chemical characterization of manganese oxide and graphene-manganese oxide films for potential applications in energy store devices,” *Results in Materials*, vol. 22, p. 100574, Jun. 2024. [Online]. Available: <https://doi.org/10.1016/j.rinma.2024.100574>
- [21] A. Eftekhari, Y. M. Shulga, S. A. Baskakov, and G. L. Gutsev, “Graphene oxide membranes for electrochemical energy storage and conversion,” *International Journal of Hydrogen Energy*, vol. 43, no. 4, pp. 2307–2326, Jan. 2018. [Online]. Available: <https://doi.org/10.1016/j.ijhydene.2017.12.012>
- [22] A. Joy, G. Unnikrishnan, M. Megha, M. Haris, J. Thomas, A. Deepti, P. Baby Chakrapani, E. Kolanthai, and S. Muthuswamy, “A novel combination of graphene oxide/palladium integrated polycaprolactone nanocomposite for biomedical applications,” *Diamond and Related Materials*, vol. 136, p. 110033, Jun. 2023. [Online]. Available: <https://doi.org/10.1016/j.diamond.2023.110033>
- [23] A. M. Sindi, “Applications of graphene oxide and reduced graphene oxide in advanced dental materials and therapies,” *Journal of Taibah University Medical Sciences*, vol. 19, no. 2, pp. 403–421, Apr. 2024. [Online]. Available: <https://doi.org/10.1016/j.jtumed.2024.02.002>
- [24] A. Loeffen, D. E. Cree, M. Sabzevari, and L. D. Wilson, “Effect of graphene oxide as a reinforcement in a bio-epoxy composite,” *Journal of Composites Science*, vol. 5, no. 3, p. 91, Mar. 2021. [Online]. Available: <https://doi.org/10.3390/jcs5030091>
- [25] J. Zhou, Z. Yao, Y. Chen, D. Wei, Y. Wu, and T. Xu, “Mechanical and thermal properties of graphene oxide/phenolic resin composite,” *Polymer Composites*, vol. 34, no. 8, pp. 1245–1249, Jun. 2013. [Online]. Available: <http://dx.doi.org/10.1002/pc.22533>
- [26] L. Yang, F. Jia, Z. Juan, D. Yu, L. Sun, Y. Wang, L. Huang, and J. Tang, “Bioinspired graphene oxide nanofiltration membranes with ultrafast water transport and selectivity for water treatment,” *FlatChem*, vol. 36, p. 100450, Nov. 2022. [Online]. Available: <https://doi.org/10.1016/j.flatc.2022.100450>
- [27] C.-H. Yu, G.-Y. Chen, M.-Y. Xia, Y. Xie, Y.-Q. Chi, Z.-Y. He, C.-L. Zhang, T. Zhang, Q.-M. Chen, and Q. Peng, “Understanding the sheet size-antibacterial activity relationship of graphene oxide and the nano-bio interaction-based physical mechanisms,” *Colloids and Surfaces B: Biointerfaces*, vol. 191, p. 111009, Jul. 2020. [Online]. Available: <https://doi.org/10.1016/j.colsurfb.2020.111009>
- [28] H. L. Poh, F. Šaněk, A. Ambrosi, G. Zhao, Z. Sofer, and M. Pumera, “Graphenes prepared by Staudenmaier, Hofmann and Hummers methods with consequent thermal exfoliation exhibit very different electrochemical properties,” *Nanoscale*, vol. 4, no. 11, p. 3515, 2012. [Online]. Available: <https://doi.org/10.1039/C2NR30490B>
- [29] N. Zaaba, K. Foo, U. Hashim, S. Tan, W.-W. Liu, and C. Voon, “Synthesis of graphene oxide using modified Hummers method: Solvent influence,” *Procedia Engineering*, vol. 184, pp. 469–477, 2017. [Online]. Available: <https://doi.org/10.1016/j.proeng.2017.04.118>
- [30] C. Gómez-Navarro, M. Burghard, and K. Kern, “Elastic properties of chemically derived single graphene sheets,” *Nano Letters*, vol. 8, no. 7, pp. 2045–2049, Jun. 2008. [Online]. Available: <https://doi.org/10.1021/nl801384y>
- [31] K. Cao, S. Feng, Y. Han, L. Gao, T. Hue Ly, Z. Xu, and Y. Lu, “Elastic straining of free-standing monolayer graphene,” *Nature Communications*,

- vol. 11, no. 1, Jan. 2020. [Online]. Available: <https://doi.org/10.1038/s41467-019-14130-0>
- [32] S. Stankovich, D. A. Dikin, G. H. B. Dommett, K. M. Kohlhaas, E. J. Zimney, E. A. Stach, R. D. Piner, S. T. Nguyen, and R. S. Ruoff, "Graphene-based composite materials," *Nature*, vol. 442, no. 7100, pp. 282–286, Jul. 2006. [Online]. Available: <https://doi.org/10.1038/nature04969>
- [33] M. Mehrabi Kooshki and A. Jalali-Arani, "High performance graphene oxide/epoxy nanocomposites fabricated through the solvent exchange method," *Polymer Composites*, vol. 39, no. S4, Feb. 2018. [Online]. Available: <https://doi.org/10.1002/pc.24803>
- [34] B. Collins Brodie, "XIII. On the atomic weight of graphite," *Philosophical Transactions of the Royal Society of London*, vol. 149, pp. 249–259, Dec. 1859. [Online]. Available: <https://doi.org/10.1098/rstl.1859.0013>
- [35] L. Staudenmaier, "Verfahren zur Darstellung der Graphitsäure," *Berichte der deutschen chemischen Gesellschaft*, vol. 31, no. 2, pp. 1481–1487, May 1898. [Online]. Available: <https://doi.org/10.1002/cber.18980310237>
- [36] U. Hofmann and E. König, "Untersuchungen über graphitoxyd," *Zeitschrift für anorganische und allgemeine Chemie*, vol. 234, no. 4, pp. 311–336, Dec. 1937. [Online]. Available: <https://doi.org/10.1002/zaac.19372340405>
- [37] W. S. Hummers and R. E. Offeman, "Preparation of graphitic oxide," *Journal of the American Chemical Society*, vol. 80, no. 6, pp. 1339–1339, Mar. 1958. [Online]. Available: <https://doi.org/10.1021/ja01539a017>
- [38] D. C. Marcano, D. V. Kosynkin, J. M. Berlin, A. Sinitskii, Z. Sun, A. Slesarev, L. B. Alemany, W. Lu, and J. M. Tour, "Improved synthesis of graphene oxide," *ACS Nano*, vol. 4, no. 8, pp. 4806–4814, Jul. 2010. [Online]. Available: <https://doi.org/10.1021/nn1006368>
- [39] J. Chen, B. Yao, C. Li, and G. Shi, "An improved Hummers method for eco-friendly synthesis of graphene oxide," *Carbon*, vol. 64, pp. 225–229, Nov. 2013. [Online]. Available: <https://doi.org/10.1016/j.carbon.2013.07.055>
- [40] Y. Zhu, G. Kong, Y. Pan, L. Liu, B. Yang, S. Zhang, D. Lai, and C. Che, "An improved Hummers method to synthesize graphene oxide using much less concentrated sulfuric acid," *Chinese Chemical Letters*, vol. 33, no. 10, pp. 4541–4544, Oct. 2022. [Online]. Available: <https://doi.org/10.1016/j.ccllet.2022.01.060>
- [41] G. Surekha, K. V. Krishnaiah, N. Ravi, and R. Padma Suvarna, "FTIR, Raman and XRD analysis of graphene oxide films prepared by modified Hummers method," *Journal of Physics: Conference Series*, vol. 1495, no. 1, p. 012012, Mar. 2020. [Online]. Available: <http://dx.doi.org/10.1088/1742-6596/1495/1/012012>
- [42] Rattana, S. Chaiyakun, N. Witit-anun, N. Nuntawong, P. Chindaudom, S. Oaew, C. Kedkeaw, and P. Limsuwan, "Preparation and characterization of graphene oxide nanosheets," *Procedia Engineering*, vol. 32, pp. 759–764, 2012. [Online]. Available: <https://doi.org/10.1016/j.proeng.2012.02.009>
- [43] M. Sabzevari, D. E. Cree, and L. D. Wilson, "Mechanical properties of graphene oxide-based composite layered-materials," *Materials Chemistry and Physics*, vol. 234, pp. 81–89, Aug. 2019. [Online]. Available: <https://doi.org/10.1016/j.matchemphys.2019.05.091>
- [44] L.-L. Tan, W.-J. Ong, S.-P. Chai, and A. R. Mohamed, "Reduced graphene oxide-TiO<sub>2</sub> nanocomposite as a promising visible-light-active photocatalyst for the conversion of carbon dioxide," *Nanoscale Research Letters*, vol. 8, no. 1, Nov. 2013. [Online]. Available: <https://doi.org/10.1186/1556-276X-8-465>
- [45] D. Galpaya, M. Wang, G. George, N. Motta, E. Waclawik, and C. Yan, "Preparation of graphene oxide/epoxy nanocomposites with significantly improved mechanical properties," *Journal of Applied Physics*, vol. 116, no. 5, Aug. 2014. [Online]. Available: <https://doi.org/10.1063/1.4892089>
- [46] E. Aliyev, V. Filiz, M. M. Khan, Y. J. Lee, C. Abetz, and V. Abetz, "Structural characterization of graphene oxide: Surface functional groups and fractionated oxidative debris," *Nanomaterials*, vol. 9, no. 8, p. 1180, Aug. 2019. [Online]. Available: <https://doi.org/10.3390/nano9081180>
- [47] F. Ren, G. Zhu, P. Ren, Y. Wang, and X. Cui, "In situ polymerization of graphene oxide and cyanate ester-epoxy with enhanced mechanical and thermal properties," *Applied Surface Science*, vol. 316, pp. 549–557, Oct. 2014. [Online]. Available: <https://doi.org/10.1016/j.apsusc.2014.07.159>
- [48] M. S. A. Sher Shah, A. R. Park, K. Zhang, J. H. Park, and P. J. Yoo, "Green synthesis of biphasic tio<sub>2</sub>-reduced graphene oxide nanocomposites with highly enhanced photocatalytic activity," *ACS Applied Materials Interfaces*, vol. 4, no. 8, pp. 3893–3901, Jul. 2012. [Online]. Available: <https://doi.org/10.1021/am301287m>

- [49] I. O. Faniyi, O. Fasakin, B. Olofinjana, A. S. Adekunle, T. V. Oluwasusi, M. A. Eleruja, and E. O. B. Ajayi, “The comparative analyses of reduced graphene oxide (RGO) prepared via green, mild and chemical approaches,” *SN Applied Sciences*, vol. 1, no. 10, Sep. 2019. [Online]. Available: <https://doi.org/10.1007/s42452-019-1188-7>
- [50] S. Kwon, K. E. Lee, H. Lee, S. J. Koh, J.-H. Ko, Y.-H. Kim, S. O. Kim, and J. Y. Park, “The effect of thickness and chemical reduction of graphene oxide on nanoscale friction,” *The Journal of Physical Chemistry B*, vol. 122, no. 2, pp. 543–547, Oct. 2017. [Online]. Available: <https://doi.org/10.1021/acs.jpcc.7b04609>
- [51] S. Gadipelli and Z. X. Guo, “Graphene-based materials: Synthesis and gas sorption, storage and separation,” *Progress in Materials Science*, vol. 69, pp. 1–60, Apr. 2015. [Online]. Available: <https://doi.org/10.1016/j.pmatsci.2014.10.004>
- [52] S.-Y. Fu, X.-Q. Feng, B. Lauke, and Y.-W. Mai, “Effects of particle size, particle/matrix interface adhesion and particle loading on mechanical properties of particulate–polymer composites,” *Composites Part B: Engineering*, vol. 39, no. 6, pp. 933–961, Sep. 2008. [Online]. Available: <https://doi.org/10.1016/j.compositesb.2008.01.002>
- [53] S. Siraj, A. H. Al-Marzouqi, M. Z. Iqbal, and W. Ahmed, “Impact of micro silica filler particle size on mechanical properties of polymeric based composite material,” *Polymers*, vol. 14, no. 22, p. 4830, Nov. 2022. [Online]. Available: <https://doi.org/10.3390/polym14224830>
- [54] L. H. Grey, H.-Y. Nie, and M. C. Biesinger, “Defining the nature of adventitious carbon and improving its merit as a charge correction reference for XPS,” *Applied Surface Science*, vol. 653, p. 159319, Apr. 2024. [Online]. Available: <https://doi.org/10.1016/j.apsusc.2024.159319>
- [55] R. Al-Gaashani, A. Najjar, Y. Zakaria, S. Mansour, and M. Atieh, “XPS and structural studies of high quality graphene oxide and reduced graphene oxide prepared by different chemical oxidation methods,” *Ceramics International*, vol. 45, no. 11, pp. 14 439–14 448, Aug. 2019. [Online]. Available: <https://doi.org/10.1016/j.ceramint.2019.04.165>